FDTD Application of Targets Electromagnetic Scattering in Layered Space

Jiang Yan-nan[1], Zhu Si-xin[2], Wang Bin*[3], Yu Xin-hua[1]
[1]Guangxi Experiment Center of Information Science, Guilin University of Electronic Technology, Guilin 541004, China
[2]North China University of Water Resources and Electric Power, Zhengzhou 450011, China
[3]Research Institutes of Subtropical Forestry, Chinese Academy of Forestry, Fuyang 311400, China
*Corresponding author, e-mail: sy_jyn@126.com

Abstract

Finite Difference Time Domain (FDTD) was used to characterize the electromagnetic scattering (EMS) for targets in layered space. A new set of 1D modified Maxwell equations and auxiliary equations with incident angle was derived from 2D Maxwell equations and was used to compute the electromagnetic field in vertical boundary in 2D total field-scattered field (TF/SF), and thus incidence of uniform plane wave in time domain can be directly realized. In order to avoid complex Somerfield integration, the reciprocity theorem was used to simplify an extrapolation algorithm. Then the proposed algorithm and program in this paper were validated by applying them to compute the electromagnetic scattered field for targets in half-space and the radiation field for line current in layered lossy space. Finally this algorithm was used to characterize EMS for a tunnel in multi-layered space, for a tunnel open to vehicle, and for a tunnel and vehicle in lossless layered space. The results show the vehicle has a great impact on the scattering field, and the layered media surrounded the target can shield the scattering field.

Keywords: FDTD, layered space, EMS, TF/SF, reciprocity theorem

1. Introduction

Radar detection aims to identify a target by using the scattering characteristics of electromagnetic waves [1]. The commonly used algorithms for numerical simulation include FDTD, MOM and FEM.

In numerical computation of electromagnetic scattering (EMS), the difficulty level of a numerical algorithm is directly decided by the complexity of a target, which mainly includes the complexities of its appearance, structure, material quality, and background. FDTD is superior to compute EMS for such complex targets. However, in characterization of EMS for these complex problems, the complexity of background will make numerical algorithm more difficult.
The backgrounder of most scattering targets is free space, which can be processed with very mature technology [2]. In other spaces, EMS can also be computed by FDTD, which usually involves a special treatment of three major boundaries: half-space is relatively complex and can be solved indirectly by using three-wave method [3] in frequency domain. Layered space is more complex [3-8] for the incidence, reflection, transmission, and multiple resonance of wave in each layer, so it becomes more difficult to set uniform plane waves [10] and compute far scattered field.

Therefore, in this paper, FDTD was used to compute EMS for targets in layered background, and thereby a new set of 1D modified Maxwell equations and auxiliary equations was derived to compute the near field, and a method was proposed to compute the far scattered field.

2. Basic Theories

In computation of far scattering field by using FDTD, the basic theory is the processing of three major boundaries. This paper will focus on two aspects: the introduction of uniform plane waves, and the computation of far scattered field. Convolution perfectly matched layers

(CPML) absorbing boundary, which is superior in low computation resource consumption, wide application scope, high absorption, and easy realization of numerical calculation, will be used as truncated boundary [11].

2.1. Introduction of Uniform Plane Waves into Near Field

We use the FDTD scheme in 2D layered half-space (see Figure 1 in Reference [9]); the key is to simulate the reflection, transmission and multiple resonance waveforms of uniform plane waves along the total field-scattered field lateral boundary by using 1D-MFDTD. 1D-MFDTD means the FDTD algorithm obtained after the discrete of 1D modified Maxwell equations, which is the 1D Maxwell equations with incident angle θ. A new set of 1D modified Maxwell equations and auxiliary equations can be derived as follows.

The velocity of uniform plane waves at the upmost layer is c, and then the phase speed of electromagnetic waves along x-axis is $c_x = c/\sin\theta$. For a certain field component $A(y, \xi)$, the intermediate variable ξ is related to time variable t and coordinate variable x, and satisfies:

$$\xi = t - x/c_x = t - x\sin\theta/c$$

From derivation relationship of composite functions, we get:

$$\partial A/\partial x = -\left(\sin\theta/c\right)\partial A/\partial t$$

Based on this relationship, the Maxwell equations of perpendicularly polarized wave (TM wave) pattern in rectangular coordinates can be expressed as:

$$\begin{aligned}
&\partial E_z/\partial y = -\mu\,\partial H_x/\partial t \\
&-\left(\sin\theta/c\right)\partial E_z/\partial t = \mu\,\partial H_y/\partial t \\
&-\left(\sin\theta/c\right)\partial H_y/\partial t - \partial H_x/\partial y = \varepsilon\,\partial E_z/\partial t
\end{aligned} \tag{1}$$

By deriving Equation (1), we get:

$$\begin{aligned}
&\partial H_x/\partial y = -\varepsilon_0\left(\varepsilon_r - \varepsilon_{0r}\sin^2\theta\right)\partial E_z/\partial t \\
&\partial E_z/\partial y = -\mu\,\partial H_x/\partial t \\
&H_y = -Y_0\sqrt{\varepsilon_{0r}}\,\sin\theta E_z
\end{aligned} \tag{2}$$

The three equations in Equation (2) are just the 1D modified Maxwell equations and auxiliary equations match TM wave, where ε_{0r} is the relative dielectric constant of the medium in the upmost layer; ε_r is the relative dielectric constant at the computed place, its representation is related to the type of medium [2]. Furthermore, it satisfies $Y_0 = \sqrt{\varepsilon_0/\mu_0}$.

From the first two equations (namely 1D modified Maxwell equations) in scattered Equation (2), we can obtain a 1D-MFDTD iterative formula, and thereby simulate the field components E_z and H_x in each layer in the 2D TF/SF lateral boundary. Then with assistance of the third equation, we can obtain H_y, and by projection and interpolation in time axis, we can get the field in TF/SF transverse boundary. Finally, we obtain all necessary field components, so as to introduce uniform plane wave into 2D FDTD computation. 1D modified Maxwell equations and auxiliary equations for paralleled polarized wave (TE wave) pattern can be derived in the similar way.

2.2. Far Scattered Field Computation

After we obtain near field, in order to avoid complex Somerfield integration, the reciprocity theorem is used here to simplify near-far field extrapolation. For TM waves, far scattered field can be expressed as:

$$E_{ff\phi}^{s} = \frac{1}{I_{\phi}} \iint_{l'} \left(E_{t,z}^{\phi} I_{z} - H_{t,x}^{\phi} K_{x} - H_{t,y}^{\phi} K_{y} \right) dl' \tag{3}$$

Where I_{ς} and K_{ς} are the equivalent electric and magnetic current along direction ς on the near-to-far-field boundary, respectively; I_{ϕ} is far test electric current in infinite length, whose near radiation field can be divided into $E_{t,z}^{\phi}$, $H_{t,x}^{\phi}$ and $H_{t,y}^{\phi}$, and the incident field E_{i} in the upmost layer of near field is expressed as:

$$E_{i} = I_{\phi}\omega\mu\sqrt{j/(8k_{0}\pi r)}e^{-jk_{0}\cdot r}e_{z} \tag{4}$$

For simplicity, we usually set $I_{\phi}=1$. In the upmost layer (No. 0), the amplitude of the incident field stimulated by far infinite electric current I_{ϕ} can be calculated from Equation (4) to be E_{i}, and the complement of the included angle θ between incident direction and y-axis (incident angle) is φ_{i}; the electromagnetic field components of all layers are successively expressed as [4]:

$$
\begin{aligned}
E_{t,zm}^{\phi} &= E_{i}\left(A_{m}e^{u_{m}y} + B_{m}e^{-u_{m}y}\right)e^{v_{m}x} \\
H_{t,xm}^{\phi} &= \frac{E_{i}}{Z_{TM_{m}}}\left(A_{m}e^{u_{m}y} - B_{m}e^{-u_{m}y}\right)e^{v_{m}x} \\
H_{t,ym}^{\phi} &= \frac{jv_{m}E_{i}}{\omega\mu_{m}}\left(A_{m}e^{u_{m}y} + B_{m}e^{-u_{m}y}\right)e^{v_{m}x}
\end{aligned}
\tag{5}
$$

Where A_m and B_m are the complex amplitudes of incident and reflected waves, respectively; u_m and v_m are the propagation constants along y- and x-axis in each layer, respectively, and can be expressed as:

$$
\begin{aligned}
v_{m} &= \gamma_{m}\cos\varphi_{m} = \gamma_{0}\cos\varphi_{i} = v_{0} \\
u_{m} &= \gamma_{m}\sin\varphi_{m} = \sqrt{\gamma_{m}^{2} - \gamma_{m}^{2}\cos^{2}\varphi_{m}} = \sqrt{\gamma_{m}^{2} - \gamma_{0}^{2}\cos^{2}\varphi_{i}}
\end{aligned}
$$

Note that $\gamma_{m} = jk_{m} = j\omega\sqrt{\mu_{m}\varepsilon_{m}}$ is the propagation constant along propagation direction in layer m, and transversal wave impedance Z_{TMm} is expressed as $Z_{TMm} = j\omega\mu_{m}/u_{m}$.

After A_m and B_m at varying angle φ are determined [4], the field of the test current at any position in layered space can be obtained from Equation (5). In combination with equivalent electromagnetic current at extrapolated boundary and Equation (3), we can obtain the far EMS field of a target in complex layered space. TE wave pattern can be analyzed in the same way.

3. FDTD Implementation and Numerical Results

Case 1: Compute the scattered field for a target in half-space, thereby validate the algorithm of introducing uniform plane wave into near field, and validate the theory in computation of far scattered field: for the model used to validate the algorithm, refer to Figure 13 in Reference [3]; its background is layered space, which is the simplest; the upper layer is free space, and the lower layer has a relative dielectric constant $\varepsilon_r = 2.56$. When an infinite medium wedge is placed on the medium interface, its relative dielectric constant is ε_w, the wedge's inclined plane has an elevation angle of 60°, and a short side of 4 m in right angle. Perpendicularly polarized uniform plane waves are entering the medium interface at an incident angle of 135°.

(a) Near electric field without wedge   (b) Near electric field with wedge
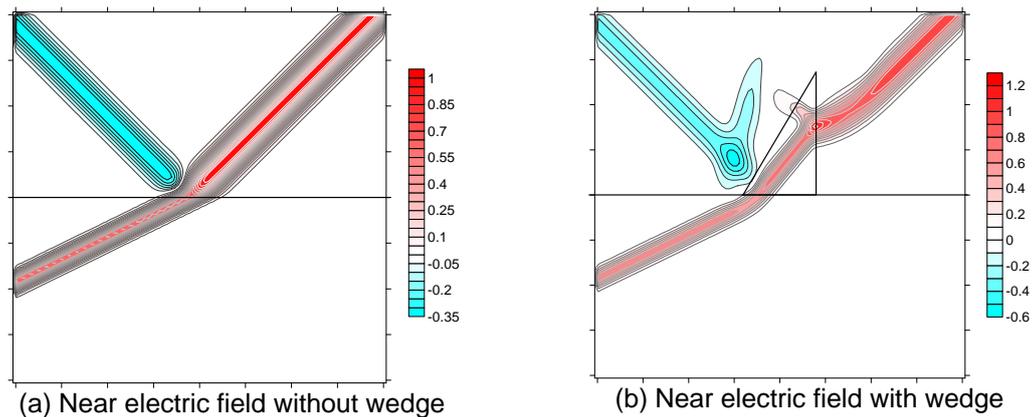
Figure 1. Near Electric Field Distributions

First, Gaussian pulse with normalized amplitude enters a half-space without wedge, so we can investigate the introduction effect of uniform plane waves and the near field distribution. The near field distribution at certain time (Figure 1(a)) shows apparently that the incident wave, reflected wave and transmission wave all be uniform plane waves, but they have different amplitudes, only because of reflection and transmission. Figure 2(a) shows the electric field time-domain waveforms monitored in half-space, where the solid and dashed lines represent the waveforms at points (0, +7.5m) and (0, -7.5m), respectively. Figure 2(a) also shows that in the upper half-space, the incident wave with normalized amplitude arrives first, followed by reflected waves on interface, whose amplitude is consistent with the theoretical reflection coefficient $\Gamma = -0.34$. The two peaks appear at an interval of 35.3 *ns*, which is consistent with the time needed by electromagnetic wave to disseminate at the phase speed $c/\sin 45^\circ$. The lower half-space only shows transmission waves, whose amplitude is also consistent with the theoretical transmission coefficient $\tau = 0.66$; since transmission waves are disseminated at a low speed, it will arrive at the monitoring points later than when the reflected waves arrive at (0, +7.5m). Analysis shows that, uniform plane wave can be reliably introduced into near field.
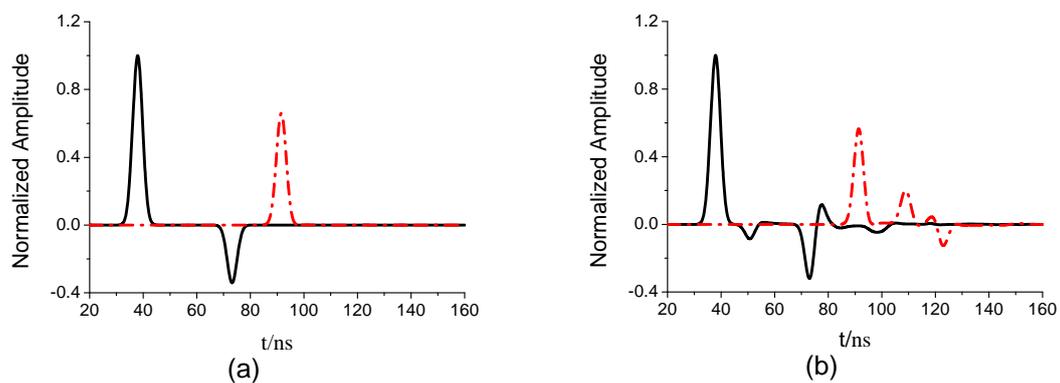

Figure 2. The Electric Field Time Domain Waveforms at Monitoring Points (Solid and dashed line are the waveforms at (0, +7.5m) and (0, -7.5m), respectively. (a) The electric field time-domain waveforms at monitoring points in pure half-space; (b) The electric field time-domain waveforms at monitoring points in half-space with wedge)

Besides, the near field distribution in half-space with wedge (ε_w = 2.56) was also calculated. At the same time step, the mixed fields overlapped by near incidence field and scattered field, and the time-domain waveforms at the monitoring points (0, +7.5m) and (0, -7.5m) are showed in Figure 1(b) and Figure 2(b), respectively. The wedge's scattering effect

distorts the incidence, reflection and transmission of uniform plane waves, which is reflected in the monitored electric field time-domain waveforms. Figure 1 shows that, the electric field value of the half-space with wedge exceeds the range of the pure half-space: the minimum in (b) exceeds the range in (a), because when uniform plane waves enter an optically denser medium (lower half-space and wedge) from an optically thinner medium (free space), the two reflections at half-space interface and the wedge's inclining plane are overlapped; The maximum exceeds the range because when electromagnetic waves enter an optically thinner medium (free space) from an optically denser medium (wedge), they are overlapped with incident waves.

Then we will validate the far field algorithm. When ε_w =2.56 or ε_w =5, far scattered field computations at 300 MHz are showed in Figure 3(a) and(b), which are consistent with Reference [3], indicating the algorithm in this paper for far scattered field is correct.

(a) Far scattered field when ε_w =2.56

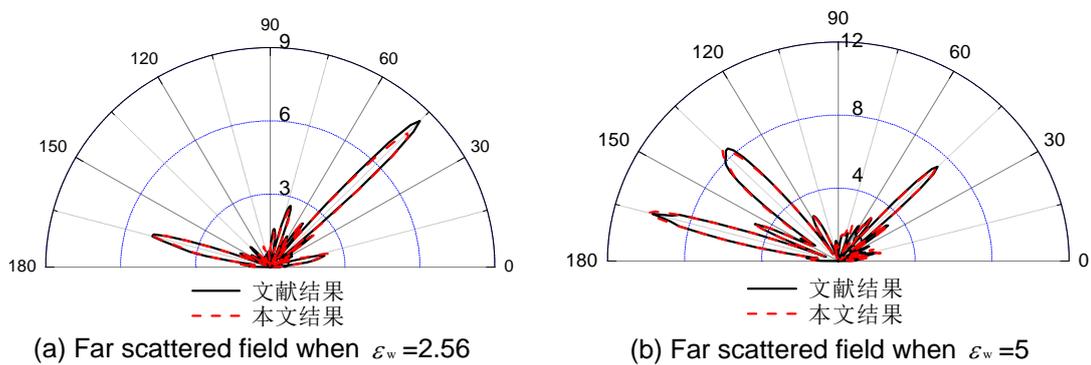(b) Far scattered field when ε_w =5

Figure 3. Far Scattered Field to Wedge (Solid and dashed lines are the results in Reference [3] and the results in this paper)

Case 2: Compute and analyze the far radiation field of line current and the far scattered field of target in lossy multilayered space.

In the layered half-space model, the area $y>0$ is a free space, the area $y<0$ includes 46 layers of lossy media, where the undermost layer is infinitely deep and each other layer is 0.1m thick; the middle 45 layers have relative dielectric constants linearly changing from 2.0 to 4.0 from up to down, with a conductivity of 0.001S/m; the undermost layer has the same medium parameters as the layer above.
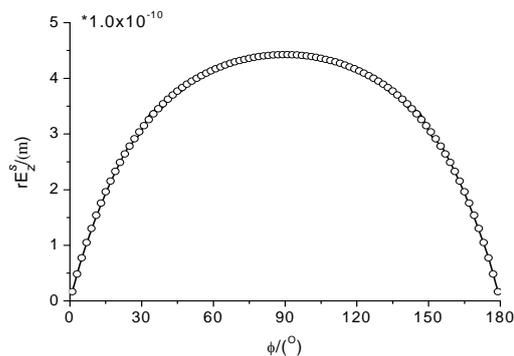

Figure 4. Far Radiation Field in Lossy Multilayered Space (Solid line and circle are the results to analytic and FDTD method, respectively)
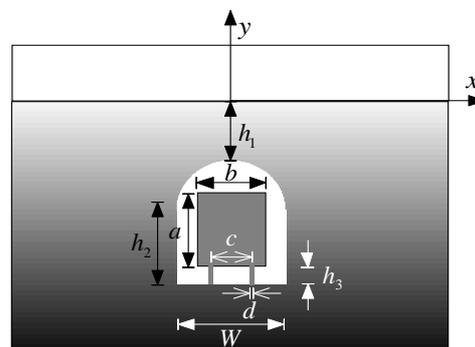
Figure 5. A Layered Half-space Model whose Tunnel is Open to Metal Vehicle Body

First, when an infinitely long line current is set at 1.5m deep from ground, the proposed FDTD method and the analytic method in Equation (3) were used to calculate far radiation field in the upper half space. The relationship between far radiation longitudinal electric field and azimuth at 300MHz is showed in Figure 4, where the solid line and circle represent the analytic and FDTD method, respectively; the two methods are very consistent, which verifies the accuracy of FDTD.

The far scattered field is considered in the following models: there is a tunnel in the 46-layer lower half space, with a semicircular arched structure on top and a rectangular shape in lower part; the tunnel is open to metal vehicle body. Its top is h_1=1.0m above ground; the rectangular structure is in dimensions of h_2=2.0m and w=3.0m; a metal vehicle body has dimensions as: a=2.2m, b=2.0m, wheel height h_3=0.3m, wheel base c=1.4m, and wheel width d=0.1m (Figure 5).
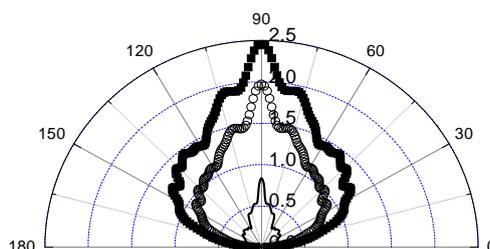

Figure 6. Far Scattered Fields with the Presence of Tunnel and with Metal Vehicle Body Inside (Solid line, empty circle, and solid frame are the results to the tunnel model in lossy background, open-to-traffic tunnel model in lossy background and open-to-traffic tunnel model in lossy-free background, respectively)

Perpendicularly polarized uniform plane wave at 300MHz is incoming along *y*-axis. Under three conditions: the presence of tunnel, the presence of metal vehicle body inside, and the tunnel and the metal vehicle body in a lossy-free layered half-space, and then the far scattered fields are computed and represented by solid line, empty circle, and solid frame, respectively in Figure 6. Clearly, due to the symmetry of the model's structure and the plane wave's incident direction, the far scattered field is in symmetric distribution along the 90° direction. Due to the presence of metal car body, the far scattered field is augmented quickly, indicating the large contribution of metal car body to the far scattered field. The backward lossy layer is relatively the thinnest, which makes the backward far scattered field the strongest; also due to the difference of conductivity in the layered space media that surrounds the tunnel, a target's scattered field is smaller in a lossy background than in a lossy-free background.

4. Conclusion

First starting from the addition mechanism of uniform plane waves, and from the near-to-far-field boundary used in near-far field extrapolation, we derived a new set of 1D modified Maxwell equations and auxiliary equations, as well as the algorithm for computation of far scattered field, and then we characterized the electromagnetic scattering of targets in layered background.

Then from near field and far field, the reliabilities of the algorithm and program proposed in this paper were validated. Case 1 shows that, the proposed algorithm can produce a good near uniform plane wave distribution; the far scattered field calculated by the new algorithm was consistent with other literatures. Case 2 shows that the far radiation field of line current calculated by the new algorithm and by the analytic method in Equation (3) were consistent. Therefore, the algorithm and program in this paper are accurate and effective.

Finally, the electromagnetic scatterings in multilayered space with the presence of tunnel and with the presence of vehicle body inside were characterized. Clearly, the metal vehicle body has a large contribution to the far scattered field, and the lossy medium layer can shield the targets effectively.

Acknowledgements

References

[1] Li Ting-jun, Yang Hai-ning, Zhao Qing, et al. Development of a single-borehole radar for well logging. *TELKOMNIKA Indonesian Journal of Electrical Engineering*. 2012; 10(8): 1985-1991.
[2] Allen T, Susan CH. *Computational electrodynamics the finite-difference time-domain method* (3rd ed.), Artech House, USA. 2005.
[3] Wong PB, Tyler GL, Baron JE, et al. A three-wave FDTD approach to surface scattering with applications to remote sensing of geophysical surfaces. *IEEE Transactions on Antennas and Propagation*. 1996; 44(4): 504-514.
[4] Demarest K, Plumb R, Huang Zhu-bo. FDTD Modeling of Scatterers in Stratified Media. *IEEE Transactions on Antennas and Propagation*. 1995; 43(10): 1164-1168.
[5] Demarest K, Huang Zhu-bo, Plumb R. An FDTD near- to far-zone transformation for scatterers buried in stratified grounds. *IEEE Transactions on Antennas and Propagation*. 1996; 44(8): 1150-1157.
[6] Winton SC, Kosmas P, Rappaport CM. FDTD Simulation of TE and TM Plane Waves at Nonzero Incidence in Arbitrary Layered Media. *IEEE Transactions on Antennas and Propagation*. 2005; 53(5): 1721-1728.
[7] Jiang Yan-Nan, Ge De-Biao, Ding Shi-Jing. Analysis of TF/SF boundary for 2D-FDTD with plane p-wave propagation in layered dispersive and lossy media. *Progress In Electromagnetics Research*. 2008; PIER 83: 157-172.
[8] Capoglu I R, Smith GS. A total-field/ scattered-field plane-wave source for the FDTD analysis of layered media. *IEEE Transactions on Antennas and Propagation*. 2008; 56(1): 158-169.
[9] Chen Peng-hui, Xu Xiao-jian. Introduction of Oblique Incidence Plane Wave to Stratified Lossy Dispersive Media for FDTD Analysis. *IEEE Transactions on Antennas and Propagation*. 2012; 60(8): 3693-3705.
[10] Simorangkir Roy BVB, Munir A. Numerical design of ultra-wideband printed antenna for surface penetrating radar application. *TELKOMNIKA Indonesian Journal of Electrical Engineering*. 2011; 9(2): 341-350.
[11] Roden JA, Gedney SD. Convolutional PML (CPML): an efficient FDTD implementation of CFS-PML for arbitrary media. *Microwave and Optical Technology Letters*. 2000; 27(12): 334-339.